

Monopole clusters at short and large distances

V.G. Bornyakov,^{1,*} P.Yu. Boyko,^{2,†} M.I. Polikarpov,^{2,‡} and V.I. Zakharov^{3,§}

¹*Institute for High Energy Physics, Protvino 142284, Russia*

²*Institute of Theoretical and Experimental Physics,*

B. Chermushkinskaya 25, Moscow, 117259, Russia

³*Max-Planck Institut für Physik, Föhringer Ring 6, 80805, München, Germany*

We present measurements of various geometrical characteristics of monopole clusters in $SU(2)$ lattice gauge theory. The maximal Abelian projection is employed and both infinite, or percolating cluster and finite clusters are considered. In particular, we observe scaling for average length of segments of the percolating cluster between self-crossings, correlators of vacuum monopole currents, angular correlation between links along trajectories. Short clusters are random walks and their spectrum in length corresponds to free particles. At the hadronic scale, on the other hand, the monopole trajectories are no longer random walks. Moreover, we argue that the data on the density of finite clusters suggest that there are long-range correlations between finite clusters which can be understood as association of the clusters with two-dimensional surfaces, whose area scales.

I. INTRODUCTION

The interest in monopoles in non-Abelian gauge theories is mostly due to the dual superconductor mechanism of the confinement, for review see [1]. The mechanism assumes condensation of magnetic monopoles in the vacuum. The idea is supported by the lattice data and the phenomenology of the lattice monopoles is quite rich. Especially, in case of $SU(2)$ gluodynamics which we will concentrate on in this paper.

Detailed theoretical interpretations of the data appear, however, difficult because monopoles are defined not directly in terms of the original $SU(2)$ fields but rather in terms of projected fields. The use of a projection is rooted in the fact that monopoles are intrinsically $U(1)$ objects and there are infinitely many ways to select a $U(1)$ subgroup for the monopole definition. In particular, monopoles of the maximal Abelian projection (MAP) are defined in the following sequence of steps (which we describe in a somewhat simplified way). First, one finds the maximal Abelian gauge maximizing the functional:

$$R_{Abel} = \int d^4x \left[(A_\mu^1(x))^2 + (A_\mu^2(x))^2 \right] \quad (1)$$

where $A_\mu^a(x)$ are components of the gauge field. Finally, monopoles are defined as singularities of the $A_\mu^3(x)$ fields which violate the Bianchi identities:

$$j_\mu^{mon}(x) = \epsilon^{\mu\nu\rho\sigma} \partial_\nu \partial_\rho A_\sigma^3(x) \ , \quad (2)$$

where $j_\mu^{mon}(x)$ is the monopole current and all the expressions are well defined on the lattice.

Geometrically, monopoles are represented by closed trajectories (on the dual lattice) and one usually discusses

properties of the monopole clusters. In particular, it is important to distinguish between the percolating cluster and finite clusters. The percolating cluster fills in the whole of the lattice and is in a single copy for each field configuration. Finite clusters are characterized, in particular, by their spectrum as function of the length l . Commonly, one introduces the corresponding densities of the percolating and finite clusters:

$$l_{perc} \equiv 4 \rho_{perc} a^4 N_{sites} \ , \quad l_{fin} \equiv 4 \rho_{fin} a^4 N_{sites} \ , \quad (3)$$

where l_{perc}, l_{fin} is the total length of the corresponding clusters, N_{sites} is the number of lattice sites and a is the lattice spacing.

An important question is whether position of the monopoles is of any physical significance. On one hand, monopole trajectories are distinguished by singularities of the projected fields, see (2), and they are point like in terms of the projected fields. On the other hand, one can suspect that these singularities are artifacts of the projection.

Probably, a priori the latter possibility looks more reasonable since the monopole definition involves a non-local gauge fixation, see (1). However, there are accumulating lattice data which indicate that in the maximal Abelian gauge the monopoles, which by construction have size of the lattice spacing a , are physical. In particular, the density of the percolating monopoles scales:

$$\rho_{perc} = 0.65(2) \sigma_{SU(2)}^{3/2} \ , \quad (4)$$

where $\sigma_{SU(2)}$ is the string tension [21] and we quoted the data from Ref. [2] where references to earlier papers can also be found.

Let us emphasize that the result (4) implies that the corresponding monopole trajectories are meaningful even on the scale a . Indeed, the total length of the percolating clusters which scales in the physical units is added up from small steps of size a and finally is independent on a . Thus, one could argue, see, e.g., [3], that there are gauge invariant objects which are detected through the

*Electronic address: bornvit@sirius.ihep.su

†Electronic address: boyko@itep.ru

‡Electronic address: polykarp@heron.itep.ru

§Electronic address: xxx@mppmu.mpg.de

projection. It is of course an intriguing hypothesis which is worth to be thoroughly checked. Unfortunately, this suggestion cannot be scrutinized theoretically since the anatomy of the lattice monopoles in terms of the non-Abelian fields is largely unknown, for review see, e.g., [4]. Rather one should apply further phenomenological tests.

In particular, one can measure non-Abelian action associated with the monopoles, see [5] and references therein. For monopoles in the percolating clusters it turns out that, at least at presently available lattices, the action corresponds to a monopole mass which diverges in the ultraviolet:

$$M(a) \sim \frac{\text{const}}{a} . \quad (5)$$

$M(a)$ is the lattice analog of the ‘magnetic mass’ in the continuum, $M(a) \sim \int \mathbf{H}^2 d^3r$ where \mathbf{H} is the magnetic field. The result (5) strongly suggests that the lattice monopoles are associated with singular non-Abelian fields and the singularity (2) is *not* an artifact of the projection.

The next question is how singular fields can be important at all since their contribution in the limit $a \rightarrow 0$ is suppressed by an infinite action [22]. An apparent answer to this question is that the action and entropy factor are both divergent in the ultraviolet but cancel each other in such a way that, say, the total density of monopoles in the percolating cluster scales in the physical units, see (4). An example of such a fine tuning is provided by $U(1)$ theory, see, in particular, [6]. In that case the fine tuning is ensured by choosing tuned values of the electric charge. In case of non-Abelian theories the hypothesis on the fine tuning [7, 8] is rather phenomenological and the mechanism of the fine tuning is to be understood yet.

To summarize,

(1) there is evidence that at presently available lattices the monopoles defined within the maximal Abelian projection are associated in fact with singular non-Abelian fields fine tuned to the corresponding entropy factors.

(2) This means that the structure of the non-perturbative vacuum fluctuations is quite different from the standard picture of ‘bulky’ fields of the size Λ_{QCD}^{-1} .

(3) Although the conclusion on the fine tuning is strongly suggested by the data like (4), (5) further checks of it are highly desirable. Indeed, the whole basis is the phenomenology of the lattice monopoles and further data can bring further insight.

Motivated by these considerations, we have investigated in more detail the scaling properties of the monopole clusters [23]. The outline of the paper is as follows. In Sect. II we present detailed studies of the geometrical elements of the percolating cluster. Namely, the cluster consists of self-crossings and segments between the crossings. We report on the measurements of distribution in the length of the segments, long-range correlations between directions of the links occupied by monopole currents, scaling properties of the segments

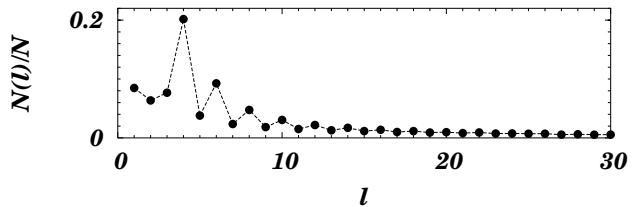


FIG. 1: The distribution $N(l)/N$, $\beta = 2.4$, the lattice size is 24^4 .

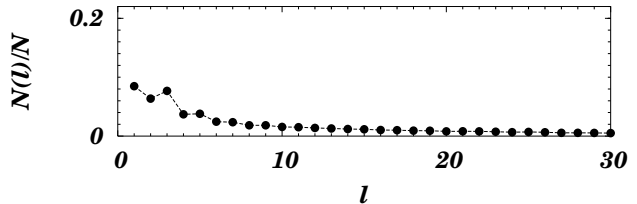


FIG. 2: $N(l)/N$ for trajectories which are not closed loops; β value and the lattice size are the same as in Fig.1

characteristics. In Sect. III we first present data on the spectrum of the finite size clusters (subsection III A) and then on their density (subsection III B). In subsection III C we present results on the correlations of the monopole trajectories at large distances which are sensitive, at least in principle, to the glueball masses. Discussions of the observations made in this work are in Sect. IV. Finally, some details of simulations are given in the Appendix.

II. SEGMENTS OF THE PERCOLATING CLUSTER

A. Distribution in the segments length

The percolating cluster consists of segments (that is, trajectories between crossings) and crossings. The segments, in turn, are made from the links on the dual lattice. We will consider the length of the segment, l_{segm} and the Euclidean distance between the end points of the segments, d .

In Fig. 1 we show the normalized distribution, $N(l)/N$, of the lengths of the segments; $N(l)$ is the number of the segments with the length l in lattice units, N is the total number of segments.

The oscillations of $N(l)/N$ are clearly seen, the number of trajectories with the even l is systematically larger than that with the odd l . This effect is due to the large number of the closed trajectories (loops), which are segments with $d = 0$ and $l \neq 0$. In Fig. 2 we show $N(l)/N$ only for not closed trajectories, $d \neq 0$.

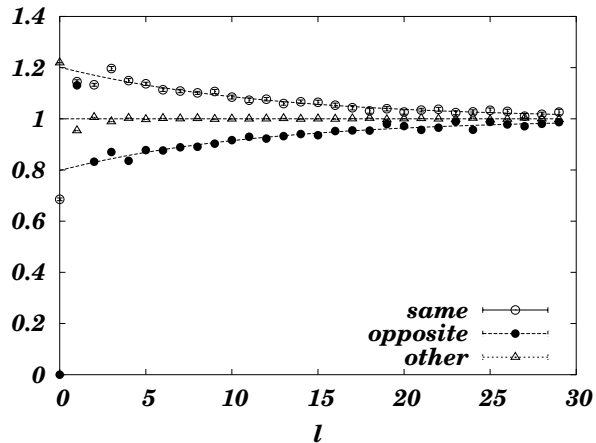


FIG. 3: Correlations of the directions of the links lying on the monopole current; $\beta = 2.6$, the lattice is 28^4 .

The oscillations are substantially reduced compared with Fig. 1.

B. Long-range correlation between links directions

Next, we turn to angular correlation between the links on the monopole trajectory. Let us call link C_0 belonging to the percolating cluster as the "initial" one. Then one can measure the probability that the link C_l , connected to the link C_0 by the monopole trajectory of length l , has the same direction. Of course this probability is a decreasing function of l , but it occurs that there exists a "long memory" of the initial direction. This fact is illustrated in Fig. 3 where the correlation of the direction of the initial link C_0 with the direction of the link C_l is shown. The direction of C_l can be the same as that of C_0 , or opposite, or else (neither the same nor the opposite). We normalize all three probabilities in such a way that they are equal to unity for random walk if $l \neq 0$ (for $l = 0$ the opposite direction is forbidden). From Fig. 3 it is seen that even for links separated by 17 lattice steps the most probable direction is the same as the direction of the initial link. For smaller values of β the correlations of the directions exist for not so large values of l . The deviation from unity of the probability to have the same direction falls off exponentially: $P_{same} = 1 + A_s e^{-\mu_s l a}$. The probability to have the opposite direction behaves as follows: $P_{opposit} = 1 - A_o e^{-\mu_o l a}$. These fits are shown by dashed lines in Fig. 3. The masses μ_s and μ_o coincide within the error bars and are independent of the lattice spacing, see Table I.

TABLE I: The fitted masses from data for $P_{same} - 1$ and $1 - P_{opposit}$

β	2.45	2.50	2.55	2.60
μ_s , MeV	290(60)	290(20)	271(15)	273(12)
μ_o , MeV	250(60)	240(20)	252(15)	277(15)

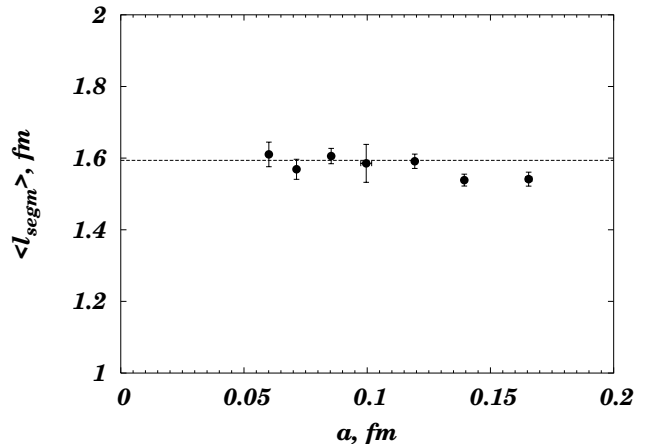


FIG. 4: Average segment length, $\langle l_{segm} \rangle$, vs. lattice spacing.

C. Scaling properties of the segments

It was already mentioned in the Introduction that the density of the percolating cluster scales, that is ρ_{perc} has a well defined value in the continuum. Here we will present further data on the scaling properties of geometrical elements of the percolating cluster.

First, we observe that the average length of the segment of the monopole trajectory between crossings, $\langle l_{segm} \rangle$, does not depend on the lattice spacing, see Fig. 4. Making fit by a constant for $\beta > 2.35$ we obtain

$$\langle l_{segm} \rangle = 1.60(1) \text{ fm}.$$

The way used to convert lattice results into physical units is explained in Appendix. The lattice spacing values a for various β 's are also given in Appendix, see Table III.

In the average Euclidean distance between the crossings $\langle d \rangle$ the violations of the scaling are more significant, see Fig. 5. However, the deviations from the scaling can be approximated for $\beta > 2.35$ by linear in a corrections. Then in the continuum limit $a \rightarrow 0$, $\langle d \rangle$ has a non-vanishing value ($\approx 0.20 \text{ fm}$), as it is seen from Fig. 5.

In Fig. 6 the number of crossing points per unit length of the monopole trajectory is shown by open circles. This number weakly depends on a and seems to have the continuum limit ($a \rightarrow 0$) $\approx 0.3 \text{ fm}^{-1}$.

The situation changes if we exclude the closed loops of finite lattice length connected to the percolating cluster.

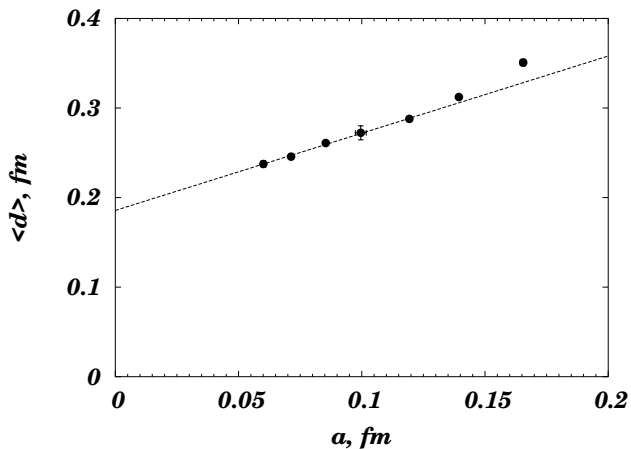


FIG. 5: $\langle d \rangle$ vs. lattice spacing. The dashed line shows the linear fit for $\beta > 2.35$.

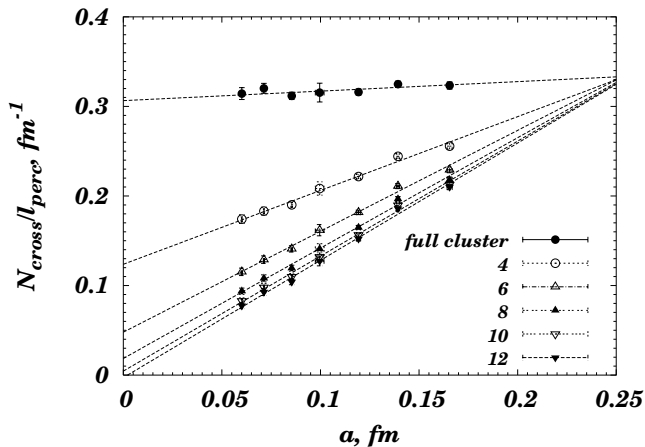


FIG. 6: Number of crossings per unit physical length vs. lattice spacing in full percolating cluster and in the percolating cluster with excluded closed loops. Numbers 4, 6, ...12 in the legend mean that closed loops of the length up to 4, 6, ...12 are excluded. The dashed lines show the linear fits.

The number of crossings reduces and is compatible with zero in the continuum limit if we exclude the loops of the length up to 8 (or up to larger length). This fact is illustrated in Fig. 6.

The continuum limit value $\langle N_{cross} \rangle / l_{perc} = 0.3 fm^{-1}$ for the full percolating cluster together with the data for the percolating cluster density (Fig. 8) corresponds to approximately 10 crossings in percolating cluster per hypercube $1 fm^4$. To complete the picture of the structure of the percolating monopole cluster in the continuum limit the data for $\langle l_{segm} \rangle$, $\langle d \rangle$ and $\langle N_{cross} \rangle / l_{perc}$ can be compared with the average monopole radius $\langle \rho_m \rangle \approx 0.05 fm$ and average inter-monopole distance $\langle R \rangle \approx 0.5 fm$ [5].

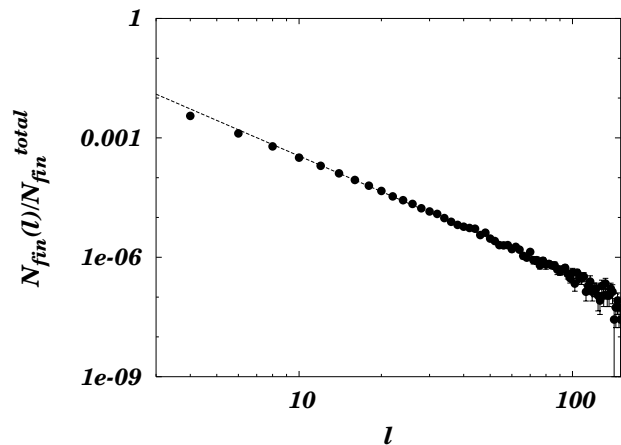


FIG. 7: The length distribution of finite clusters. $\beta = 2.4$, the size of the lattice is 32^4 .

III. FINITE CLUSTERS

A. Length spectrum of finite clusters

In Fig. 7 we show the number of the finite clusters of the length l (in the lattice units) vs. l . The dashed line in this figure is the fit of the data by function $Const/l^\alpha$. It is important that $1/l^3$ behavior seems to be valid for all considered values of the lattice spacings as it can be seen from Table II where we show results of the fit for various β values. As we discuss in Section IV C the dependence $1/l^3$ means that finite clusters develop in the four-dimensional space.

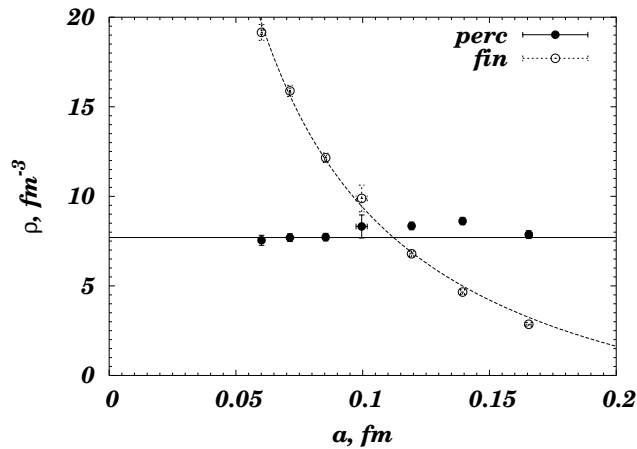
B. Monopole densities

As we discussed in the introduction the magnetic monopole clusters fall into two different classes [3, 10]: "small", or finite clusters which have finite size in lattice units, and "large" clusters which percolate through the lattice. It was demonstrated [3] that the percolating cluster is responsible for the string tension. If the size of the lattice is large enough, there is a natural distinction between "small" and "large" clusters, since in each configuration there exists only one cluster which is much longer than all others and there is a gap in the cluster length distribution [3]. If the lattice size is not large enough the percolating cluster decays into one or more large clusters plus several monopole currents which wind through the boundaries of the lattice [2]. It occurs that the monopole density for the sum of these large clusters and the winding trajectories scales [2]. We simply call this collection of the monopole currents as percolating cluster.

In Fig. 8 we show the monopole density ρ_{perc} as a function of the lattice spacing a . Our results for ρ_{perc}

β	2.30	2.35	2.40	2.40	2.40	2.45	2.50	2.55	2.6
L	16	16	16	24	32	24	24	28	28
α	3.12(4)	3.10(4)	2.98(2)	2.95(2)	2.970(16)	2.91(3)	3.02(3)	3.06(3)	3.11(4)

TABLE II: Length spectrum of finite clusters, power fit parameter

FIG. 8: Density of the finite clusters ρ_{fin} and percolating clusters ρ_{perc} ; solid and dashed lines, are fits by a constant and Eq.(7) respectively.

obtained with higher statistics than in [2] agree within error bars with values obtained in [2] for coinciding values of β on a is rather weak and we fit it by a constant for $\beta > 2.35$. The resulting density of the percolating monopoles in the continuum limit is

$$\rho_{perc} = 7.70(8) fm^{-3} . \quad (6)$$

This value is shown by the solid line in Fig. 8. It is in agreement with value obtained in [2] within error bars.

The density of the finite clusters, on the other hand, is divergent for $a \rightarrow 0$ and it can be fitted (dashed curve on Fig.8) as

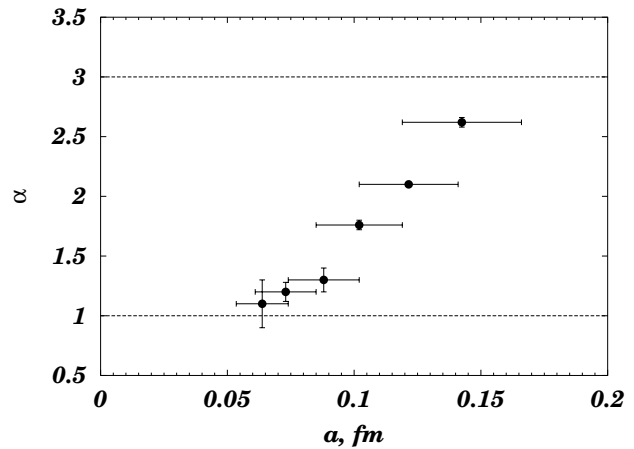
$$\rho_{fin} = C_1 + \frac{C_2}{a}, \quad (7)$$

where

$$C_1 = -6.1(5) fm^{-3}, \quad C_2 = 1.55(4) fm^{-2}.$$

The negative value of the constant C_1 means that the fit is not valid for large values of the lattice spacing.

We made also the local fits of ρ_{fin} by function $A \cdot a^{-\alpha}$, where A and α are fit parameters. The fit results for α are shown in Fig. 9. To get a point on this figure used for the fit three neighbor data points in Fig. 8. Corresponding fit intervals are depicted in Fig. 9 as X axes error bars. It can be seen from Fig. 9 that the values of α are changing from the value close to 3 down to the value approximately

FIG. 9: The dependence $\alpha(a)$.

equal 1, i.e. at small a this fit becomes consistent with the fit Eq.(7).

Another possible fit, suggested in Ref. [3], $\rho_{fin} = A \cdot a^{-\alpha}$ gives A and α strongly dependent on a , see Fig. 9. However, at smallest a we have the same $1/a$ behavior of the density.

C. Correlator of the monopole currents

We turn now to discussion of correlation functions of the monopole currents. We will consider three definitions:

- $G_1(x-y)$ is the probability that point x and point y are connected by a monopole trajectory.
- $G_2(x-y)$ is the probability that point x and point y are connected by a monopole line belonging to the percolating cluster.
- $G_3(x-y)$ is the probability that the monopole current crosses point x and point y .

Since the small clusters have finite size in the lattice units (see Sect. III A) the functions $G_1(x-y)$ and $G_2(x-y)$ coincide with each other for large $d = |x-y|$. The asymptotic behavior for $d = |x-y| \rightarrow \infty$ is similar for all correlation functions and was suggested first in [11] (see also [12]):

$$G_k(x-y) \rightarrow C_k + A_k \exp\{-m_k d\}, \quad (8)$$

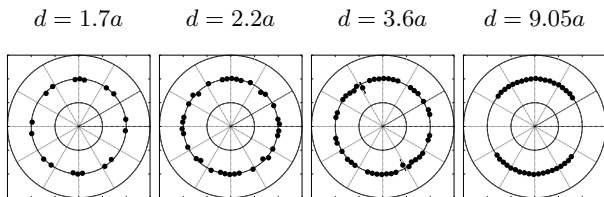


FIG. 10: Polar plots for $G_3(d)$ at $\beta = 2.3$, the lattice size is 16^4 .

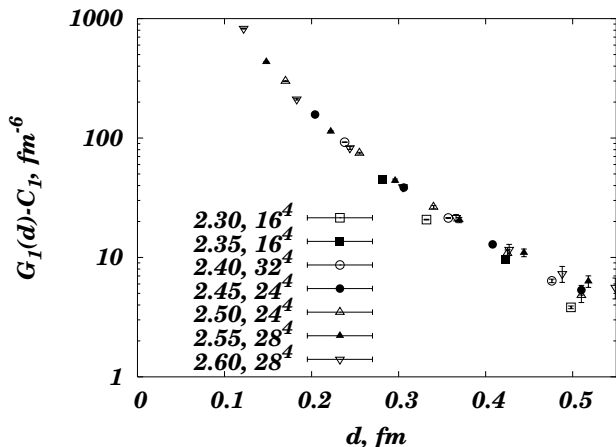


FIG. 11: The scaling behavior of the correlation function $G_1(d)$. The constant C_1 has been subtracted.

where $k = 1, 2, 3$ and m_k are expected to be the mass of the lightest glueball. Moreover, since by definition (see (3)) the monopole density is the probability to find the monopole current on the given link, the constants C_k are equal to the squares of the corresponding densities. It is obvious that $C_{1,2} = (\rho_{perc})^2$ and $C_3 = (\rho_{perc} + \rho_{fin})^2$.

The results of the measurements are presented in Figs. 10, 11. In Fig. 10 we show the results of the rotational invariance check of the correlators G_k at large enough d . Namely, the dependence of $G_3(x - y)$ on the angle between 4-vector $x - y$ and one (arbitrary) axis in polar coordinates is shown. For illustrative purposes, we use different normalizations of G_3 on different plots in Fig. 10. The data show nice rotational invariance. Note that the gap in the angles seen for large d is due to the geometry of the lattice.

One of the most important properties of the correlators is their scaling. The data do indicate that the correlators do have the scaling behavior. This is illustrated in Fig. 11, where we show $G_1(d)$ in physical units for various β . Note that the dimension of ρ is fm^{-3} . Respectively, the dimension of the correlation functions G_k is fm^{-6} and they are sensitive to possible scaling violations. Comparing the data for various volumes at $\beta = 2.4$ we found the lattice volume independence of the correlators $G_k(d)$.

Finally, we determined the masses m_k in Eq. (8). The fits made for the distance $d > 0.3$ fm show that the masses m_k do have scaling behavior, but we do not have the high precision in their determination:

$$m_{1,2} = 1.87(16) \text{ GeV}, \quad m_3 = 2.4(5) \text{ GeV}.$$

Due to large errors we can claim only that the results do not contradict the prediction that m_k coincide with the mass of the lightest $SU(2)$ 0^{++} glueball as measured, in particular, in Refs. [13].

IV. PERCOLATION LAWS AT SHORT AND LARGE DISTANCES

In preceding sections we presented data on the phenomenology of the monopole clusters and have chosen to postpone comments on their implications till this section. It might worth emphasizing from the very beginning that not every piece of information that we got has a straightforward interpretation. Moreover, it is useful to distinguish between the properties of the clusters at relatively short distances, $\Lambda_{QCD}^{-1} \gg l \gg a$ where l is the length along the monopole trajectory, and at large distances $l \geq \Lambda_{QCD}^{-1}$. As we shall see, it is the short distance behavior which is quite well understood while for larger distances one could rather speak of accumulation of the data. This might look paradoxical since traditionally the non-perturbative fluctuations are deprived of interesting short-distance behavior.

A. Monopoles as free particles at short distances

One of our main results is observation of scaling for a few observables :

- average distance between the self-crossings of the percolating cluster, as measured along the trajectory, scales (see Fig. 4);
- average Euclidean distance between the same points approximately scales, see Fig. 5;
- correlation length of direction alignment of links along the trajectory of the percolating cluster scales, see Table I;
- correlators of the vacuum monopole currents scale, as illustrated in Fig. 11;
- we confirm scaling of the density of the percolating cluster, see Fig. 8.

Each of these checks is highly non-trivial since the most natural explanation of any scaling behavior is that the monopoles of size a are physically meaningful. Thus, each example of the scaling behavior confirms, at least indirectly, fine tuning of the lattice monopoles.

Now, let us discuss briefly the geometry of the monopole cluster at various distances. At the very short distances, of order a , monopole trajectories can be thought of as (approximate) random walk. At these distances both the action and the entropy are of order $1/a$. Let us illustrate this statement by a well known equation (see, e.g., [14]) for the propagating mass of a scalar particle m_{prop}^2 :

$$m_{prop}^2 \cdot a \approx \left(M(a) - \frac{\ln 7}{a} \right) , \quad (9)$$

$M(a)$ is the field theoretical mass of the same particle, discussed in the Introduction on the monopole example. A more general definition of $M(a)$ is that the action of the particle is

$$S_{cl} = M(a) \cdot l ,$$

where l is the length of a path connecting two points between which the particle propagates. Moreover, the $\ln 7$ factor is due to the entropy. Eq. (9) is derived in the approximation of neglecting neighboring trajectories. Note a dramatic difference between $M(a)$ and m_{prop} . Namely, to ensure a finite propagating mass m_{prop} one needs an ultraviolet divergent mass $M(a)$ (that is, the mass which determines the classical action).

Upon accounting for possible cancellations between the action and entropy one can introduce an ‘effective action’,

$$S_{eff} = l \cdot \mu , \quad (l \gg a) ,$$

which governs the behavior of the trajectories at distances much larger than a . The very fact that the density of the percolating cluster scales implies that at distances of order a the divergent factors in the action and entropy cancel each other and $\mu \sim \Lambda_{QCD}$. This is just the fine tuning hypothesis which we heavily rely on.

Eq. (9) is useful for orientation in mass scales which came out from various fits to the data. In particular fits to the correlation of the links resulted in the attenuation factor of order $\exp(-\mu_s l)$ where μ_s is about 300 MeV and l is measured along the trajectory, see Table I. At first sight, 300 MeV might look too low a mass. However, if we apply for estimates Eq. (9) we would obtain rather $m_{prop}^2 \sim (300 \text{ MeV})/a$. In other words, we do have evidence that the most singular part of the action (as measured on the lattice, see the Introduction) is indeed cancelled by the entropy factor. But the value $\mu_s \approx 300 \text{ MeV}$ does not necessarily corresponds directly to a physical mass.

Once this cancellation is confirmed by the data, one can make predictions about short clusters with the length $\Lambda_{QCD}^{-1} \gg l \gg a$ [8]. Namely, at such length one can neglect the mass factor and the spectrum of the closed loops should correspond to free particles. Then one can derive (see [8] and references therein):

$$N(l) \sim \frac{const}{l^3} , \quad R(l) \sim \sqrt{l} , \quad (10)$$

where $R(l)$ is the radius of the cluster of the length l . Let us emphasize that (10) is a consequence of free field theory in Euclidean space-time (actually, in $d = 4$ Eq. (10) survives adding Coulomb like interaction as well [8]). Eq. (10) is derived most naturally in the so called polymer representation, see, e.g., [8, 15].

Measurements of $N(l)$ and $R(l)$ were reported in [3] and are in perfect agreement with (10). Our analysis confirms (10) on larger statistics and for smaller values of a . In particular, the data on the l distribution are summarized in the Table II. We did not include the data on the $R(l)$ which we have but they do confirm (10) for all a tested.

B. Percolating cluster

Existence of a single infinite cluster is typical for all percolating systems in the supercritical phase, see, e.g., [16]. There is a general theorem on the uniqueness of the percolating cluster at $p > p_c$ where p is the probability to have a link ‘open’ (in our case, to belong to a monopole trajectory) and p_c is the point of the phase transition. The percolating cluster is characterized by the probability $\theta(p)$ of a given link to belong to the cluster (in our case this probability is equal to the cluster density, ρ_{perc}). Generically, $\theta(p) \sim (p - p_c)^\beta$, $\beta > 0$. In our case,

$$\theta(p) \sim (a \cdot \Lambda_{QCD})^3 \ll 1 . \quad (11)$$

Smallness $\theta(p)$ implies closeness to the point of phase transition to the percolation. In the limit $a \rightarrow 0$ we hit exactly the point of phase transition. Expression (11) can be considered as formulation of the hypothesis on fine tuning of the monopoles in terms of the percolation theory.

Another general property of the percolating cluster is that its fractal dimension coincides with the dimension of the space:

$$D_{fr}^{perc} = d . \quad (12)$$

Which is trivially satisfied in our case, since the length of the percolating cluster is proportional to the whole volume, V_4 .

However, to the best of our knowledge, the percolation theory is not powerful enough to predict or explain the data which we have on such characteristics as l_{segm} , d .

It is worth emphasizing that geometrical characteristics of the percolating cluster at length of order $\langle l_{segm} \rangle$ differ quite drastically from the corresponding characteristics of the finite clusters. First of all, the monopole trajectories are no longer random walks. Indeed, for a random walk we would have had:

$$l \approx \frac{1}{2} \frac{d}{m_{prop} \cdot a} , \quad (13)$$

where l is the distance between two points measured along the trajectory and d is Euclidean distance between the same points.

Our results on l_{segm} and d are given in Fig. 4 and 5, respectively. The data certainly rule out (13) for any finite m_{prop} . Moreover if we assume that it is only the leading power of $1/a$ which is cancelled in Eq. (9) then $m_{prop} \sim \sqrt{\Lambda_{QCD}/a}$. Our data are not consistent with (13) for such mass either.

Also, existence of correlation between directions of the links, (see Sect. II B), could not be reconciled with the random walk.

C. Long-range correlation of finite clusters

Turn now to discussion of the data on the density of the short clusters, see Sect. III B. Expectations for ρ_{fin} are easy to formulate. Indeed, the spectrum $N(l) \sim l^{-3}$ implies that the average length of the finite clusters is saturated in the ultraviolet, i.e. at length of order a . Then the density of the finite clusters should not depend on Λ_{QCD} at all and on the dimensional grounds $\rho_{fin} \sim a^{-3}$.

Instead, we find that the most singular piece in the density $\rho_{fin} \sim \Lambda_{QCD}^2 \cdot a^{-1}$. The only interpretation of this striking observation is that even short, or finite clusters are not independent at large scales. Again, on dimensional grounds alone it is clear that the finite clusters are in fact associated with two-dimensional surfaces whose area scales.

At first sight, this conclusion looks too bizarre. However, in fact it is known to be true from independent measurements on the P-vortices. Namely, it was observed first in Ref. [17] that monopoles are associated predominantly with P-vortices, whose total area scales. This conclusion was recently reinforced by measurements for smaller lattice spacings [18].

Thus, we are invited to think about percolation of monopoles as a two-step process: monopoles percolate on the surface of dimension $d = 2$ and the surface itself percolates in $d = 4$ space-time. As far as we know, this type of percolation has not been studied theoretically at all. And we can, therefore, suggest only very preliminary considerations.

First the probability $\theta(p)$, see Eq. (11) is to be thought of as a product of two factors:

$$\theta(p) \sim (a \cdot \Lambda_{QCD})^3 \sim (a \cdot \Lambda_{QCD}) \cdot \frac{V_2}{V_4}, \quad (14)$$

where the first factor is to be interpreted as a power of $(p^{(2)} - p_c^{(2)})$ for percolation of monopoles on a surface while the second factor accounts for suppression of the ‘phase space’ available on a $d = 2$ space, V_2 , as compared to the whole lattice volume V_4 . Note that for probabilities defined on the surface we still have according to (14)

$$(p^{(2)} - p_c^{(2)}) \sim (a \cdot \Lambda_{QCD}) \ll 1, \quad a \rightarrow 0.$$

Another major change, is that finite clusters now occupy a finite fraction of the links on the surface. Furthermore, one could also speculate that for finite monopole clusters of length $l \sim \Lambda_{QCD}^{-1}$ we would still have

$$R \sim l^{1/d} \sim \sqrt{l}, \quad d = 2$$

As the last remark, let us notice that the interplay between the monopole trajectories and P-vortices is more complicated than simply saying ‘monopoles belong to P-vortices’. Indeed, for short clusters the length spectrum is sensitive to the dimension of the space [8, 15]:

$$N(l) \sim \frac{1}{l^{d/2+1}}, \quad (15)$$

and the spectrum $\sim l^{-3}$ corresponds to $d = 4$. In this sense, at short distances the monopole trajectories are ‘primary’ objects. Thus, one can expect that for larger l where the infrared behavior of the clusters sets in the spectrum is changed into $1/l^2$.

V. CONCLUSIONS

There is accumulated evidence that monopoles defined within the Maximal Abelian projection appear physical even if studied with resolution of the lattice spacing a . In particular, we have seen that there are amusingly simple scaling laws for various observables which depend only on the product $(a \cdot \Lambda_{QCD})$ and look perfectly gauge-invariant. Thus, non-perturbative fluctuations in the lattice $SU(2)$ appear to have non-trivial structure in the ultraviolet as well as in the infrared.

What is specific for the field, is that phenomenology seems to be far ahead of theory. In particular, we have argued that there are indications that percolation of the monopoles is to be considered as combination of percolation of the trajectories over a surface $d = 2$ and of percolation of the surface over the $d = 4$ space. To the best of our knowledge, no theoretical framework is available to describe such a percolation.

Acknowledgements

The authors are thankful to M. Müller-Preussker for contribution at the initial stage of this work. We are obliged to F.V. Gubarev, M.N. Chernodub, A.V. Kovalenko and S.N. Syritsyn for numerous fruitful discussions. V. G. B., P. Yu. B. and M. I. P. are partially supported by grants RFBR 02-02-17308, RFBR 01-02-17456, DFG-RFBR 436 RUS 113/739/0, INTAS-00-00111 and CRDF award RPI-2364-MO-02.

β	2.30	2.35	2.40	2.40	2.40	2.40	2.45	2.50	2.55	2.60
a (fm)	0.1655(13)	0.1394(8)	0.1193(9)	0.1193(9)	0.1193(9)	0.1193(9)	0.0996(22)	0.0854(4)	0.0713(3)	0.0601(3)
L	16	16	16	24	28	32	24	24	28	28
# of conf.	100	100	300	137	14	35	20	50	40	50

TABLE III: $SU(2)$ configurations

Appendix

The list of configurations used in this work is given in Table III. To fix the Maximal Abelian gauge we use the Simulating Annealing algorithm [19] and study 10 randomly generated gauge copies for each configuration to avoid the Gribov copy problem.

Most of the quantities in the paper are given in physical units (*e.g.* in fm). In order to express the lattice data in physical units we use the data of Refs. [20] for the $SU(2)$ string tension and assume that $\sqrt{\sigma} = 440 MeV$. The corresponding values of the lattice spacing are given in Table III.

-
- [1] M.N. Chernodub, M.I. Polikarpov, in 'Cambridge 1997, Confinement, duality, and nonperturbative aspects of QCD', p. 387; [hep-th/9710205](#).
- [2] V. Bornyakov and M. Müller-Preussker, *Nucl. Phys.* **B106** (2002) 646.
- [3] A. Hart and M. Teper, *Phys. Rev.* **D58** (1998) 014504; *Phys. Rev.* **D60** (1999) 114506.
- [4] S. Coleman, in "The Unity of the Fundamental Interactions", Erice lectures, 1981, ed. A. Zichichi, Plenum, London (1983) p. 21; M.N. Chernodub, F.V. Gubarev, M.I. Polikarpov, V.I. Zakharov, *Phys. Atom. Nucl.* **64** (2001) 561, *Yad. Fiz.* **64** (2001) 615, ([hep-th/0007135](#)).
- [5] B.L.G. Bakker, M.N. Chernodub and M.I. Polikarpov, *Phys. Rev. Lett.* **80** (1998) 30; V.G. Bornyakov, F.V. Gubarev, M.I. Polikarpov, T. Suzuki, A.I. Veselov and V.I. Zakharov, *Phys. Lett.* **B537** (2002) 291.
- [6] A.M. Polyakov, *Phys. Lett.* **B59** (1975) 82; T. Banks, R. Meerson, J. Kogut, *Nucl. Phys.* **B129** (1977) 493.
- [7] V.I. Zakharov, "Hidden mass hierarchy in QCD", [hep-ph/020404](#).
- [8] M.N. Chernodub, V.I. Zakharov, "Towards understanding structure of the monopoles clusters", [hep-th/0211267](#).
- [9] P.Yu. Boyko, M.I. Polikarpov and V.I. Zakharov, "Geometry of percolating monopole clusters", [hep-lat/0209075](#).
- [10] S. Kitahara, Y. Matsubara and T. Suzuki, *Progr. Theor. Phys.* **93**, 1 (1995); M. Fukushima, A. Tanaka, S. Sasaki, H. Suganuma, H. Toki and D. Diakonov, *Nucl. Phys. Proc. Suppl.* **53**, 494 (1997).
- [11] T. L. Ivanenko, M. I. Polikarpov and A. V. Pochinsky, *JETP Lett.* **53** (1991) 543 [*Pisma Zh. Eksp. Teor. Fiz.* **53** (1991) 517]; T. L. Ivanenko, A. V. Pochinsky and M. I. Polikarpov, *Phys. Lett.* **B302** (1993) 458.
- [12] K. Langfeld, H. Reinhardt, "Monopole - anti-monopole excitation in MAG projected $SU(2)$ lattice gauge theory", [hep-lat/0206021](#).
- [13] C. Michael and M. Teper, *Nucl. Phys.* **B305** (1988) 453; C. Michael and S. Perantonis, *J. Phys.* **G18** (1992) 1725; S. Booth et al (UKQCD), *Nucl. Phys.* **B394** (1993) 509.
- [14] J. Ambjorn, "Quantization of geometry", [hep-th/9411179](#).
- [15] A.M. Polyakov, "Gauge Fields and Strings", Harwood academic publishers, (1987).
- [16] C. Itzykson, J.-M. Drouffe, "Statistical Field Theory", vol. 1, Cambridge University Press, (1989); D. Stauffer, A. Aharony, "Introduction to percolation theory" London et al.: Taylor and Francis 1994; G. Grimmett, "Percolation" Berlin et al.: Springer 1999, Grundlehren der mathematischen Wissenschaften, Vol. 321.
- [17] J. Ambjorn, J. Giedt, J. Greensite, *JHEP* **9903** (1999) 019, [hep-lat/9903023](#).
- [18] F.V. Gubarev, A.V. Kovalenko, M.I. Polikarpov, S.N. Syritsyn, V.I. Zakharov, "Fine tuned vortices in lattice $SU(2)$ gluodynamics", [hep-lat/0212003](#).
- [19] G. S. Bali, V. Bornyakov, M. Muller-Preussker and K. Schilling, *Phys. Rev.* **D54** (1996) 2863.
- [20] J. Fingberg, U. M. Heller and F. Karsch, *Nucl. Phys. B* **392** (1993) 493. [hep-lat/920812](#) G. S. Bali et.al. *Int.J.Mod.Phys.* **C4** (1993) 1179-1193 [hep-lat/9308003](#) G. S. Bali, K. Schilling, A. Wachter *Phys.Rev. D* **55** (1997) 5309-5324 [hep-lat/9611025](#) G. S. Bali, K. Schilling, C. Schlichter *Phys.Rev. D* **51** (1995) 5165-5198 [hep-lat/9409005](#) B. Lucini, M. Teper *JHEP* 0106 (2001) 050 [hep-lat/0103027](#)
- [21] In estimates we will also use Λ_{QCD} although we study actually $SU(2)$ gluodynamics, $\sigma_{SU(2)} \sim \Lambda_{QCD}^2$.
- [22] Hereafter we tacitly assume that the a dependence observed at the presently available lattices will persist at smaller lattice spacings as well. The smallest a available now is about $a \approx (3 GeV)^{-1}$.
- [23] The preliminary numerical results were presented at the "Lattice 02" conference [9].